On the mutual penetrations of two gases submitted to the Richtmyer-Meshkov instability: Part 1 - experiments

L. Houas, G. Jourdan, V. Filpa, G. Layes, J. Giorgano, C. Amagat and Y. Burtschell

Polytech' Marseille, Département de Mécanique Energétique, IUSTI-Umr CNRS 6595
Université de Provence, Technopôle de Château-Gombert
5 rue Enrico Fermi, 13013 Marseille, France

Abstract. A shock tube experimental investigation is undertaken to study the mutual penetration of two gases, with different densities, the common interface of which is submitted to the Richtmyer-Meshkov instability. The experimental method of investigation is a high speed camera laser sheet diagnostic technique. Two couples of gases are used to illustrate both the heavy/light (air/He) and the light/heavy (air/SF_6) cases. Two simultaneous large initial perturbations, one positive and one negative, are tested for an incident shock wave Mach number in air of about 1.3. The, less than 1 micron, thin membrane which materializes the initial interface between the two test gases presents 2-D perturbations the wave number of which is close to 1 in order to rapidly reach the non-linear and turbulent regimes. The development of the perturbations is captured at the frequency of 10 kHz after the interface acceleration. Results show a strong asymmetric mutual penetration for the heavy/light case and less pronounced for the light/heavy one. Furthermore, we observe that the created spike moves very faster than the bubble in the heavy/light case and slightly faster in the light/heavy one. Finally, the light/heavy case measured perturbation amplitudes show good agreements with recent models, despite of the still unpredictable influence of the membrane.

1 Introduction

The Richtmyer-Meshkov instability ([1], [2]), which occurs when a shock wave crosses the interface separating two fluids of different densities, is of great interest in many various, applied and fundamental, domains such as the inertial confinement fusion as well as the supernova explosions or the supersonic combustion process. The present work initially falls within the framework of the inertial confinement fusion tentative, but we think that this type of experiments could leads to a better understanding of the different stages of the transition to turbulence. Indeed, the present diagnostic device allows to create turbulent flows far from walls and depending on simple physical parameters such as the shock wave Mach number, the nature and density of the gases present on both sides of the interface and the amplitude and wave length of the initial perturbations. Let us consider two gases of different densities separated by an interface which present two large perturbations, one positive and one negative, and let us observe what happens when a shock wave accelerates this interface, from the heavy gas to the light one or from the light one to the heavy gas. In order to reduce the wall boundary layer effects ([3], [4], [5]), this experimental study was performed in our new large cross section shock tube. Its original configuration allows the knowledge of the initial amplitude and wave length of the interface perturbations and, finally, using a planar laser sheet technique we expect to more precisely follow the interface contours evolution. The mechanism which

can lead to turbulent flow conditions is the baroclinic generation of vorticity due to the non collinearity of density and pressure gradients. In the present case, the density gradient comes from the perturbations initially present at the interface while the pressure gradient results from the shock wave passage across it. Most of the experimental studies undertaken in the field focuses on the light/heavy case (for example air/SF_6) because, first it is directly concerned with the inertial confinement fusion ([6], [7], [8], [9], [10]) and above all, its study is more easy to explain because the perturbation amplifies without reversing. Nevertheless, we also make efforts to investigate the case where the shock wave passes from the heavy to the light fluid (air/He). The experiments are conducted with about the same shock wave Mach number in air i.e. 1.3 for both cases. Furthermore, we follow during the same experiment, the evolution of two 2-D large perturbations distant one from the other, of about half their wave length, in order to try to observe the mutual penetration of the two test gases. The initial amplitude was about 10 to 17 mm, depending on the thin nitrocellulosic film drying after deposited on the grid.

2 Experimental set-up

The experiments are carried out in our new large cross section, 20 cm by 20 cm, shock tube [4]. Its high pressure, low pressure and experimental chamber lengths are of 1.65 m, 5 m and 0.48 m, respectively. It has been specially designed and constructed such as it allows to follow the interface distortion from its beginning, i. e. the initial shape and sizes of the perturbations, to the fully turbulent developed stage. The shock tube experimental chamber design is shown in Fig. 1. and the scheme of the diagnostic set up presented on

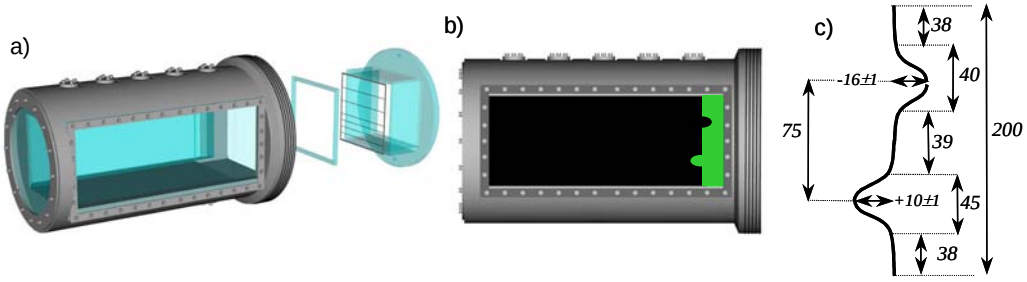

Fig. 1. Scheme of the experimental chamber a) detailed view, b) control and knowledge of the initial gaseous interface shape, c) details of the present initial conditions

Fig. 2. Concerning the diagnostic, we have developed a planar imaging because it provides more precise data than classical visualisation as shadowgraphy or schlieren methods, which give integrated views along the shock tube experimental chamber width. It consists of an Oxford copper vapor pulsed laser up to 50 kHz coupled with a rotating drum camera. This ultra rapid device allows to record, during the same run, about 100 plane frames of the phenomenon under study, spaced by 500 to 20 μs depending on the laser frequency (from 2 to 50 kHz).A laser sheet is projected horizontally through the end wall of the tube, using cylindrical optics. The sheet is centered along the test section but can be translated alongside its axis by a rotating mirror. Just before the shock, one of the test gases, air, is injected with smoke. The Mie scattering signal is collected at right

angles to the plane of the laser sheet and provides information on the mixing process due to the instability. In horizontal orientation, up today, the only one way to create a well characterized shaped interface is the use of nitrocellulose membrane put on a grid. This grid imposes the initial wavelengths and amplitudes of the perturbations and allows the fragmentation of the membrane. In the present experiments, it is a 12.5 mm square grid made of steel wires of 0.8 mm thick. In practice, we dive into the water the grid frame. After that, we set down on the plane surface of water a small amount of nitrocellulose solution. Few minutes after the polymerisation, we carefully take it out in order to sandwich it between two layers of membrane, the total thickness of which do not exceed 1 μm. With this technique, we can realize various sorts of initial conditions with large amplitude perturbations as for the present work. Note that the insert of the first and second diaphragms is very easy by the help the original close system between the driver and the driven chamber and the driven and the test chamber. The design of the experimental chamber is such as we can visualize the initial conditions before the arrival of the incident shock wave. The initial conditions of the experiments are characterized by two 2D large amplitude perturbations voluntarily chosen in order to rapidly reach the non linear and turbulent regime. Two cases have been realized at low shock wave Mach number and initial atmospheric pressure. The case where shock travels from heavy to light fluid using the air/He gas pair and the case where the shock propagates from light to heavy fluid with air/SF_6 gas combination. In each case, the first gas is air seeded with smoke in order to keep constant the incident shock wave acceleration conditions (see Table 1 for the experimental initial conditions). For the present experiments, the laser frequency is of 10 kHz (one frame per 100 μs) and the camera drum speed of 80 m/s. The pulsed copper vapor laser sheet illuminates seeded particles mixed with one of the test gases (air) and enabled a high speed, 35 mm 400 ASA film, drum camera to record an imaging sequence of the instability and mix developments. Before the run, we seed the air in the low pressure chamber during 10 mn. Three minutes later, the second gas is introduced by simple light circulation during 7 mn. Of course, during that point, we have to take care to not break the nitrocellulose membrane.

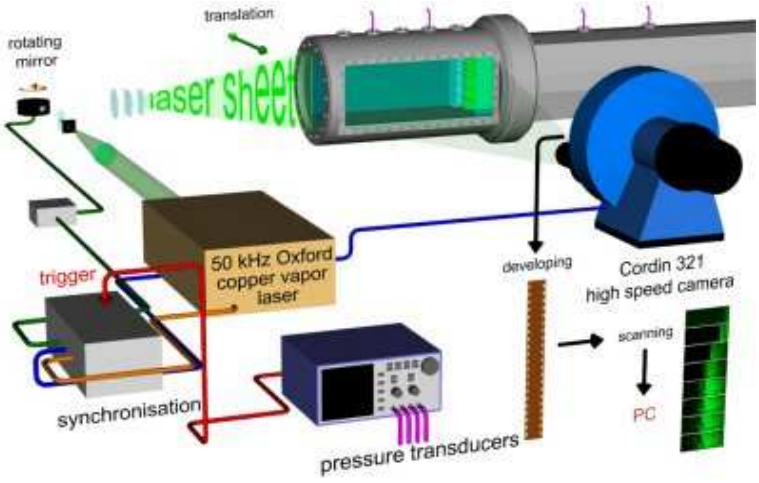

Fig. 2. Scheme of the experimental set-up

Table 1. Initial conditions, where η_0 and λ_0, represent the amplitudes and the wavelengths of the two initial perturbations (negative/positive). Ms, At and ΔU are the incident shock wave Mach number, the post-shock Atwood number and the velocity jump of the shocked interface, respectively

	$\eta_0(mm)$	$\lambda_0(mm)$	Ms	At	$\Delta U(m/s)$
air/He	-17/+10	80/90	1.3	-0.7	220
air/SF_6	-15/+11	80/90	1.3	+0.7	103

3 Results

Fig. 3 presents a sequence of laser sheet images showing the evolution of the instability in the heavy/light (air/He) and light/heavy (air/SF_6) cases, respectively. The air/He configuration (Fig. 3a) illustrates the case were the shock wave passes through a heavy/light interface and is characterized by a negative Atwood number of about -0.7. The grey part corresponds to air seeded with smoke and the black one to pure helium. The incident shock wave propagates from right to left with a Mach number of about 1.3. In this case a reversal phase occurs. Thus the initially negative perturbation became a spike of air in He and the initially positive perturbation a bubble of He in air. As we can see, the interface overturns immediately following the incident shock acceleration. Later, we observe a quickly distortion of the upper part of the interface in to mushroom structures. We can note that the development of the instability is highly dependent on the initial conditions since the two large perturbations rapidly show a non-symmetrical behavior. However, the presence of the membrane fragments in the mixing front increases the scattering of the laser light and over exposes the 400ASA film, which prevents sometimes from a precise interface contour determination. All the images were digitally processed in order, to extract the interface contours trajectories, and calculate the peak-to-peak amplitude in order to evaluate the mutual penetrations of the two gases. Fig 4a presents the peak to peak perturbation amplitude evolutions for the air/He case. As indicated on the picture, we have plotted X3-X1 as spike evolution and X3-X2 as bubble evolution. We observe that there is a strong asymmetric mutual penetration for the heavy/light case. Also, spike seems to move faster than bubble. Fig. 4b shows the bubble and spike trajectories. We observe that spike and bubble progress linearly with very different velocities. The spike velocity is close to the theoretical value of the interface velocity, calculated by considering the transmission of a shock wave through a flat air/He interface. But the bubble one is very less. It is the same after the re-shock compression. The calculated interface trajectory still remains between that of the bubble and spike. The laser sheet time sequence of the air/SF_6 interface is given on Fig. 3b. The air/SF_6 gas pair allows the study of the case where the shock wave propagates from the light to the heavier gas. It is characterized by a positive Atwood number of about +0.7. The grey part corresponds to air seeded with smoke and the black one to pure SF_6 and we can see a leak of air, through the thin membrane, on the upper part of the picture. The incident shock wave propagates from right to left with a Mach number of about 1.3. Note that in this case, SF_6 is lightly polluted by smoke which allows the visualization of both the incident and the reflected shock wave

trajectory. Given that the relatively important initial value of the perturbation amplitude, the interface quickly distorts significantly with appearance of bubble structures, until the coming back of the reflected shock wave from the shock tube end-wall, with the beginning of a phase inversion. As in the previous case, the same remarks concerning the non-symmetrical behavior and the membrane fragment scattering can be made. Fig. 5a shows the peak to peak perturbation amplitude evolutions for the light/heavy case configuration. As before, we have plotted X3-X1 as spike evolution and X3-X2 as bubble evolution. In this case, we just observe a slight asymmetric mutual penetration for the gases. Also, spike seems to move slightly faster than bubble. Furthermore, it seems that there is an influence of one perturbation on the other. After the re-shock compression we observe the reverse of the two perturbations. The trajectories of the bubble and spike are plotted on Fig. 5b. Unlike the previous case, bubble and spike linearly progress with equivalent velocities close to the theoretical value of the interface velocity, calculated by considering the transmission of a shock wave through a flat air/SF_6 interface. With the compression by the reflected shock wave, the crossing of each trajectory expresses the beginning of the inversion phase, but now, as in the heavy/light case, the spike velocity is close to the 1D flat interface calculation. Finally, we have plotted on Fig. 6 the peak to peak perturbation amplitude versus time for the light/heavy configuration (air/SF_6). The experimental data are compared with recent models developed by different authors [7], [8], [9], [10] (Fig. 6). We can see that the evolution of the bubble perturbation follows an asymptotic behavior. In such a configuration, the simple large interface perturbation is highly non-linear and the interface evolution cannot be well described by classical Richtmyer-Meshkov linear formulae. However, if we compare our experimental data with the previous recent non-linear theory, we find a relatively good agreement.

4 Conclusion

An investigation of shock induced gas mixing in a large cross section shock tube with a laser sheet technique has been undertaken for 2D large interface perturbations using a membrane technique in the heavy/light and light/heavy case. In the present experiments, we have got better accuracy for bubble measurements than for spike. We have observed a strong asymmetric mutual penetration for the heavy/light case and less pronounced for the light/heavy one. Results show that spike moves very faster than bubble in the heavy/light case and slightly faster than bubble in the light/heavy one. First results are encouraging in spite of the extreme sensitivity to the initial conditions. For the light/heavy case comparison with existing theory show a good agreement. However, we have to improve some points. First we propose to change the geometry of perturbation and the shock wave Mach numbers until Mach 3 with an initial pressure of 0.5 atm in order to point out the compressibility effects. In this way, we have to delay the return of the reflected shock wave by the increasing of the test chamber length.

References

1. R.D. Richtmyer: Commun Pure Appl Math **23**, 297 (1960)
2. E.E. Meshkov: Izv Akad Nauk SSSR, Mekh Zhidk Gaza **4**, 151 (1969)
3. M.H. Anderson, J.G. Oakley, B.P. Puranik, R. Bonazza: 'Richtmyer-Meshkov instability of an interface prepared by removal of a sinusoidal plate'. In: *Proc 23rd Int. Symp. on Shock Wave, Forth Worth, Texas, USA, 22-27 July, 2001*, ed. by F.K. Lu, 1126-1132

4. L. Houas, G. Jourdan, L. Schwaederlé, R. Carrey, F. Diaz: Shock Waves **12**, 5, 431-434 (2003)
5. L. Houas, G. Jourdan: 'Richtmyer-Meshkov instability induced turbulent mixing study in a new shock tube apparatus by a translated laser sheet technique'. In: *Proc 23rd Int. Symp. on Shock Wave, Forth Worth, Texas, USA, 22-27 July, 2001*, ed. by F.K. Lu, 1141-1146
6. J.W. Jacobs, V.V. Krivets: 'PLIF flow visualization of the nonlinear development and transition to turbulence of Richtmyer-Meshkov instability'. In: *Proc 23rd Int. Symp. on Shock Wave, Forth Worth, Texas, USA, 22-27 July, 2001*, ed. by F.K. Lu, 1183-1189
7. O. Sadot, L. Erez, D. Oron, L.A Levin, G. Erez, G. Ben-Dor, D. Shvarts: Phys Rev Lett **80**, 1654 (1998)
8. K.O. Mikaelian: Phys Rev Lett **80**, 508 (1998)
9. U. Alon, J. Hecht, D. Ofer, D. Shvarts: Phys Rev Lett **74**, 534 (1995)
10. Q. Zhang, S. Sohn: Phys Fluids **9**, 1106 (1997)

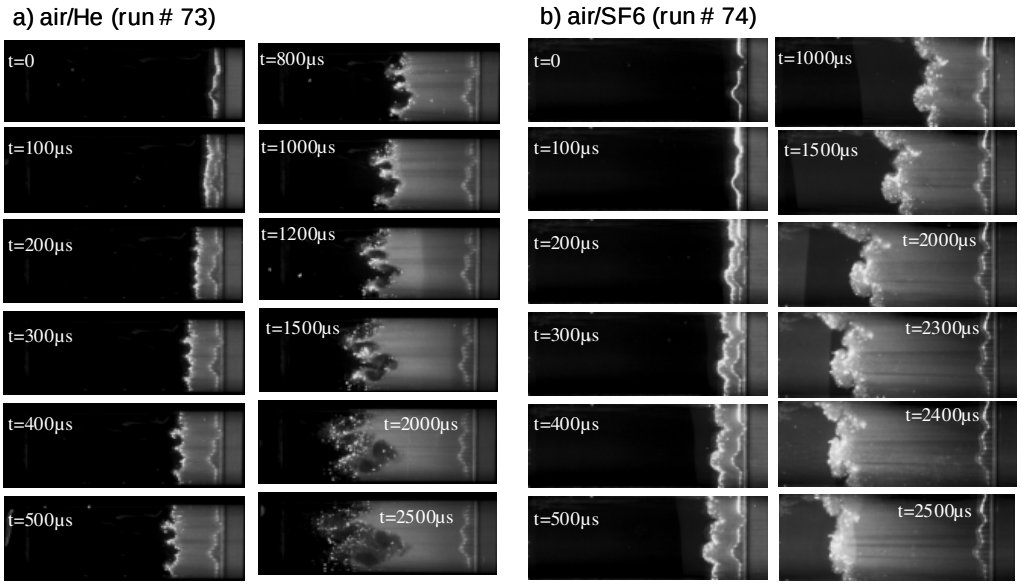

Fig. 3. Laser sheet time sequence showing the very early interaction of a shock wave (moving from right to left) with a) an air/He and b) an air/SF_6 interfaces, the further stages of the evolution of the perturbations and the compression by the re-shock

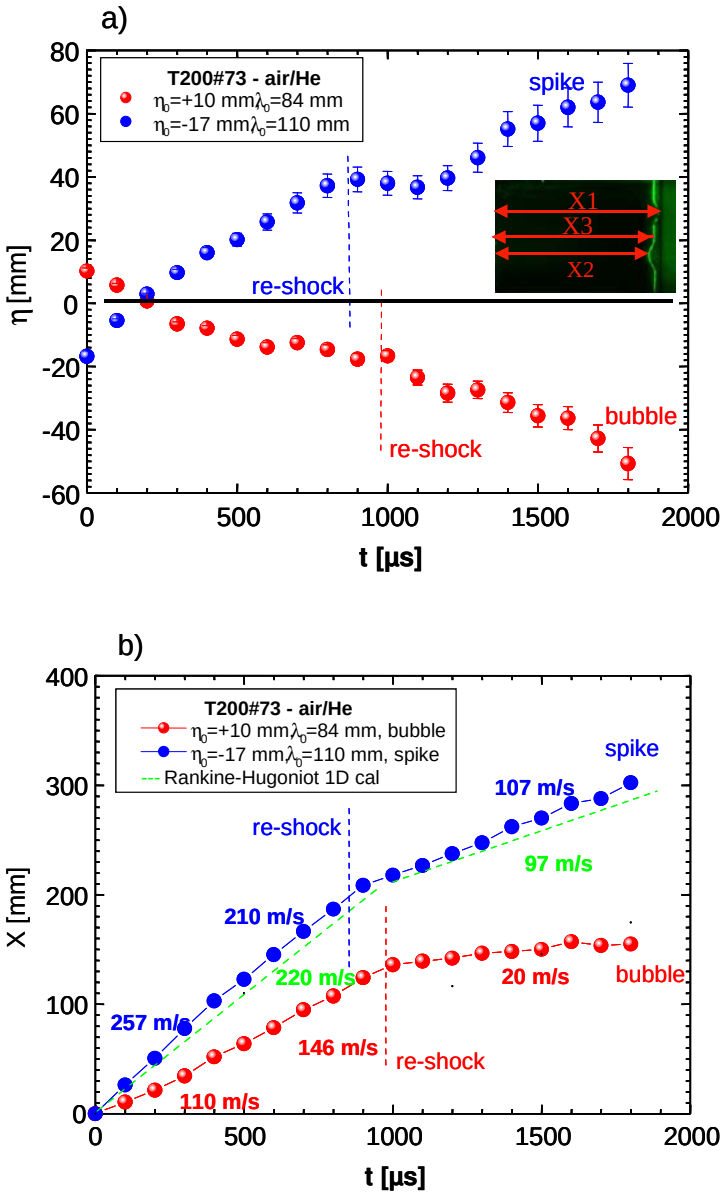

Fig. 4. Evolutions of the a) peak to peak perturbation amplitudes and b) crest and hollow displacements versus time for the air/He interface

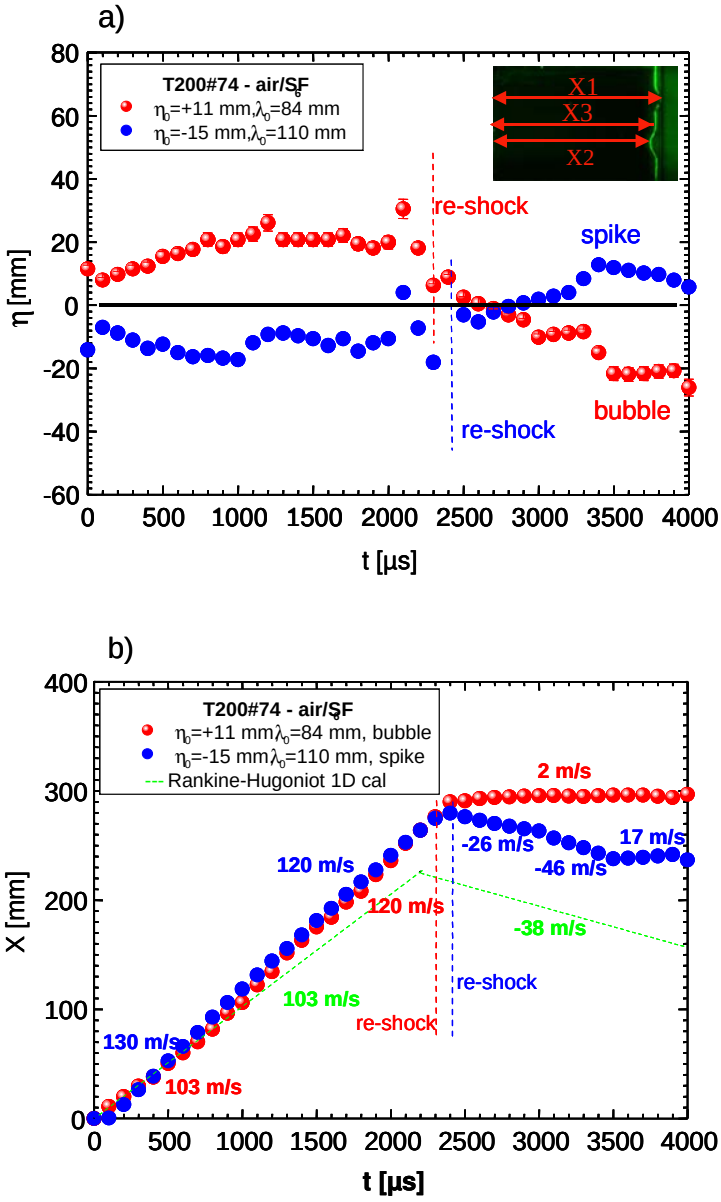

Fig. 5. Evolutions of the a) peak to peak perturbation amplitudes and b) crest and hollow displacements versus time for the air/SF_6 interface

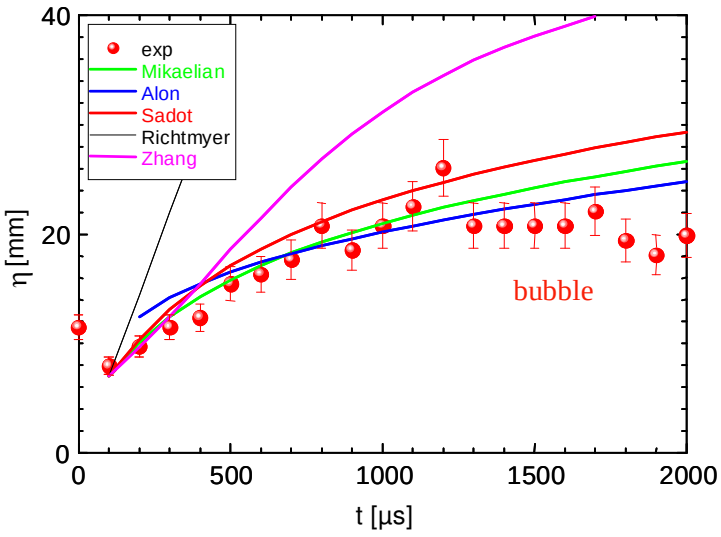

Fig. 6. Comparison of the η_0=+11 mm and λ_0=90 mm peak to peak perturbation amplitude with models from [1], [7], [8], [9], [10]